Author Version of : Estuarine, Coastal and Shelf Science, vol.242; 2020; Article no: 106864

Influence of environmental parameters on bio-optical characteristics of colored dissolved organic matter in a complex tropical coastal and estuarine region

Albertina Dias[a,b], Siby Kurian[a]*, Suresh Thyapurath[a]

[a]CSIR- National Institute of Oceanography, Dona Paula, Goa, India, 403004
[b]Goa University, Taleigao Plateau Goa, India
*Corresponding author: siby@nio.org
Phone: +91-832-2450399

Abstract

Dissolved organic matter (DOM) is an important source of carbon in aquatic ecosystems, and colored DOM (CDOM), which is smaller than 0.2 μm and interacts with ultraviolet (UV) and visible light, affects the spectral quality and quantity of light in water. In this study, the spatial and temporal variations of CDOM with changes in environmental conditions were investigated from March 2014 to May 2017 in the coastal waters and two estuaries (Zuari and Mandovi) of Goa, western India, and the major sources and sinks controlling the optical properties of these waters were identified. The CDOM absorption in the estuaries was two times higher than that of the coastal waters. It was also determined that the CDOM absorption at 412 nm (a_g412) in the coastal and estuarine waters significantly varied between seasons. The a_g412 was found to be higher in the coastal waters during the spring inter-monsoon (SIM) and fall inter-monsoon (FIM) than during the northeast monsoon (NEM). The high absorption during the SIM was of autochthonous origin, while terrigenous DOM was the primary contributor mainly during the FIM. The photobleaching of CDOM was highest during the SIM, resulting in the predominance of low-molecular-weight DOM in the coastal waters. This photobleaching of DOM also resulted in deeper UV light penetration, as indicated by the diffuse attenuation coefficient k_d at 350 nm. In the Mandovi and Zuari estuaries, higher levels of CDOM were observed during the southwest monsoon (SWM) and SIM than the FIM and NEM. The terrigenous DOM contribution was higher in the estuaries during the SWM, while phytoplankton contributed to a higher level of CDOM during the SIM. CDOM exhibited non-conservative mixing behavior in the study region, as it decreased in estuaries with lower salinities and increased at salinities between 20 and 31. Considering the importance of CDOM in the carbon cycle, this study highlights the various sources and sinks of CDOM controlling the optical properties and biogeochemical processes of coastal and estuarine waters.

Keywords: Colored dissolved organic matter; photobleaching; non-conservative mixing; autochthonous; allochthonous.

1. Introduction

Dissolved organic matter (DOM) is one of the largest sources of biologically available organic carbon in aquatic ecosystems, and its dynamics affect carbon cycling at local to global scales (Battin et al. 2009). Colored DOM (CDOM) is a complex DOM pool originating from terrestrially derived materials due to plant degradation and riverine runoff (allochthonous), and from *in-situ* production by phytoplankton, microbial remineralization, excretion, and grazing within the water body (autochthonous) (Zhang et al. 2009; Loiselle et al. 2012). CDOM is operationally defined as the optically active component of DOM present in the water that is smaller than 0.2 μm and interacts with ultraviolet (UV) and visible light. CDOM plays a major role in the spectral quality and quantity of available light in water and can have a positive or negative impact on the ecosystem. Low levels of CDOM result in deeper penetration of UV light in the water, affecting marine biota, whereas high levels of CDOM will limit penetration of visible light, hampering primary productivity (Del Vecchio and Blough, 2002). CDOM can also interfere with satellite measurements of phytoplankton biomass, which affects ecosystem models (Carder et al. 1991; Vodacek et al. 1994; Nelson and Siegel 2013). It is also an essential climate variable (ECV) that influences ocean color (Groom et al. 2019).

Rivers and estuaries are important sources of DOM during its transport from the terrestrial ecosystem to the coastal ocean. The coastal waters of Goa are affected by seasonal reversing currents with strong temperature inversions due to the transport of low-salinity water from the Bay of Bengal during the northeast monsoon (NEM) (Kumar et al. 2004). Upwellings and associated primary production lead to seasonal hypoxia/anoxia along the west coast of India during the late southwest monsoon (SWM), which impact demersal fisheries (Naqvi et al. 2000). This natural oxygen deficiency has intensified in the past few decades, which may be due to the enhanced loading of nutrients and organic matter from land (Naqvi et al. 2000, 2006). However, recent measurements show a lack of a secular trend (Naqvi et al. 2009). These waters also experience blooms of various algal species (diatoms, dinoflagellates, cyanobacteria), which are seasonal and episodic (Naqvi et al. 1998; Krishnakumari et al. 2002; Desa et al. 2005; Gomes et al. 2008; Pednekar et al. 2012), and affect the biogeochemistry of the region. The microbial remineralization of organic matter from land would also lead to CDOM production.

The SWM causes high levels of allochthonous DOM transport from watersheds into estuaries and adjoining coastal waters. The Mandovi and Zuari estuaries, located on the west coast of India, are classified as monsoonal estuaries (Manoj and Unnikrishnan 2009). During the SWM, both estuaries receive high levels of freshwater discharge, leading to stratification up to 12 km from the mouth.

There is very little discharge from river runoff during the non-monsoon season. Therefore, the estuaries become an extension of the sea and remain vertically well mixed (Shetye et al. 2007; Vijit et al. 2009). Thus, owing to the influences of both rivers and the sea, these estuaries receive autochthonous and allochthonous inputs from different sources, such as terrestrial, riverine discharge, mangrove leachate, and anthropogenic activities (Gonsalves et al. 2009).

Though CDOM plays an important role in the carbon cycle, very few studies have been conducted in the estuaries and coastal waters of Goa. Menon et al. (2011) studied CDOM in the Mandovi and Zuari estuaries using the absorption at a reference wavelength (a_g440) and slope coefficient ($S_{400-550}$). They validated the *in-situ* derived CDOM using satellite data by applying an algorithm developed for the site. Recently, Dias et al. (2017) reported the CDOM characteristics in the Mandovi and Zuari estuaries and the coastal waters of Goa; however, their study was restricted to the spring inter-monsoon (SIM) season. Therefore, the aim of this study is to investigate the variability of the bio-optical properties of CDOM with changes in environmental conditions and to identify the major sources and sinks controlling the optical properties of these waters. The following hypotheses were tested: 1) the magnitude of CDOM absorption varies both spatially and temporally in the two estuaries and the coastal waters of Goa and 2) with different sources and sinks of CDOM, the estuarine system could exhibit non-conservative mixing behavior.

2. Methods

2.1. Sampling

The measurements were carried out from the coastal waters of Goa and both the Mandovi and Zuari estuaries for three years (March 2014 – May 2017) using fishing trawlers. During 2014 - 15 the samples were collected monthly, while in the consecutive years seasonal sampling at the study area was carried out. Two coastal transects (INCOIS and CaTS) with three and four stations each were sampled off the coast of Goa, covering a depth of up to 28 m. In the Mandovi Estuary, six stations were sampled from the mouth up to 25 km upstream, while five stations were sampled in the Zuari Estuary, covering 28 km. The sampling stations in the estuary were selected keeping in mind all the sources which may contribute to CDOM. The mean depth of the estuaries was approximately 5 m (Fig. 1). Altogether, 466 samples were analyzed, 94 samples of which were collected from the CaTS transect, 71 from the INCOIS transect, 167 in the Mandovi Estuary, and 134 in the Zuari Estuary. The sampling period was classified into four seasons, i.e., the SIM (March to May), SWM (June to September), FIM (October), and NEM (November to February). The coastal waters were not sampled during the SWM due to the rough weather.

The water samples were collected in amber bottles, transported in ice and were filtered within a few hours of collection following the standard SeaWiFS protocol (Mueller et al. 2003) and their CDOM and chlorophyll-*a* contents were analyzed. For CDOM analysis, a 0.2-µm nucleopore polycarbonate membrane was first rinsed with 100 mL of Milli-Q water followed by the sample. The filtered sample was then collected in amber glass bottles. The water samples were stored at 4 °C until spectrophotometric analysis was conducted in the laboratory on the same day as collection. To analyze chlorophyll-*a,* 500 mL to 1 L of water was filtered through a 0.7-µm GF/F glass microfiber filter, which was then extracted in 10 mL of 90% acetone and analyzed using a Turner fluorometer (Knap et al. 1996). Rainwater was collected on event basis during 2015 – 16 into a glass flask using a HDPE funnel covered with a nylon mesh to prevent entry of large particles. The flask was kept at a height above the ground on the terrace of CSIR-NIO to counter the contamination by droplet splashes. The entire assembly was washed with 10% HCl and rinsed several times with milli Q water before collection to prevent contamination. This assembly was deployed for sampling as soon as the rain began and retrieved soon after the rain stopped. Samples were analysed and processed according to the methodology given, if the rainwater collected was above 50 ml. Daily average rainfall data for Goa region was provided by the Indian Metrological Department, Mumbai.

The inherent *in-situ* optical parameters of absorption, and scattering were measured using an AC-9 spectrophotometer (WetLabs, USA). The apparent optical parameters in the water column were measured *in-situ* using a free-falling profiler and a hyperspectral radiometer (Satlantic Inc, Canada).

2.2. **Spectral measurements of CDOM**

The absorption of CDOM was measured on a UV-visible Shimadzu 2600 dual beam spectrophotometer using a cuvette of 10 cm path length after the samples attain room temperature. Fresh MilliQ water from the Millipore Ultrapure water system was used as the reference for the analysis. Absorbance spectra were obtained from 250 to 850 nm range at 1 nm interval and were corrected for instrument drift and scatter using average absorbance from 700 - 850 nm (De'Grandpre et al. 1996).

Absorption by CDOM, a_g (λ) is modeled using Eqn. 1 (Jerlov, 1976), where λ_0 is a reference wavelength and S (nm^{-1}) is the spectral slope coefficient describing the relative steepness of the spectrum.

$$a_g(\lambda) = a_g(\lambda_0)\, e^{-S(\lambda-\lambda_0)} \qquad (1)$$

The absorption coefficients at the wavelengths of 320, 350, 375, 412, and 440 nm (a_g320, a_g350, a_g375, a_g412, and a_g440) were used in previous studies to represent the concentrations of CDOM (Kowalczuk et al. 2005; Yamashita and Tanoue 2009; Para et al. 2010; Vantrepotte et al. 2015). The absorption by CDOM obtained at these wavelengths was significantly correlated and varied similarly between seasons. In this study, we used a_g412 as a reference wavelength (λ_0) for the CDOM concentrations, since a_g412 is used to derive DOC (Vantrepotte et al. 2015) being the shortest wavelength available from the ocean color remote sensing observations. Spectral slope coefficient (S) was estimated using a linear fit of log-linearized $a_g(\lambda)$ spectrum (nm^{-1}) in the UV range. While non linear regression was used in the long range, wherein a background constant (k) has been applied to calculate the slope (Stedmon et al., 2003). The absorption of CDOM at reference wavelength is often accepted as a proxy for the concentration of CDOM and slope (S) for changes in the composition of CDOM, including the ratio of humic acids to fulvic acids (Carder et al. 1989; Blough and Green, 1995). Slopes derived in the narrow wavelength range of $S_{275\text{-}295}$, $S_{350\text{-}400}$, and spectral slope ratio S_R ($S_{275\text{-}295}/S_{350\text{-}400}$), were used to track changes in the molecular weight of organic matter as proposed by Helms et al. (2008). Short wavelength slope in the range 275 - 295 can be measured with better precision even in highly photobleached waters and is very sensitive to changes in molecular weight and sources of CDOM (Twardowski et al. 2004).

2.3. **Spectral analysis of detritus and phytoplankton absorption**

Particulate matter in water was concentrated on to a 25mm GF/F filter by filtering about 0.1 to 0.5 L water depending on the particle load. Filtration volume has been adjusted to keep the samples in the optical density range (0.05 - 0.4) that is ideal for the path length amplification corrections (Mitchell, 2002). The filter paper was immediately stored at -20ºC until analysis using a spectrophotometer. All the analysis were performed within 24 hrs from collection. Particulate spectral absorption was determined using an integrating sphere attached to Shimadzu UV2600 spectrophotometer. The filter papers were thawed at room temperature in dark and the spectral absorption by particulate matter (a_p) was measured at every 1nm interval from 250 to 850 nm. The same filter was then subjected to methanol extraction for 30 minutes to eliminate the absorption by phytoplankton pigments followed by rinsing with filtered (0.2 micron) seawater. The filter paper was again scanned on a spectrophotometer for determining absorption by detritus (a_d) or de-pigmented particles. For blank determination, 0.2 micron filtered seawater was filtered onto a GF/F filter paper, and the absorbance was measured. Phytoplankton pigment absorption (a_{ph}) was computed from the difference between a_p

and a_d (detrital) absorption spectra after correcting for the filter path length amplification factor (β) (Mitchel et al. 2002) following equation 2.

$$a_p(\lambda) = \frac{2.303 A_f}{\beta V_f}\left[\left(OD_{fp}(\lambda) - OD_{bf}(\lambda)\right) - OD_{null}\right] \quad (2)$$

Where $OD_{fp}(\lambda)$ is the measured optical density of the sample filter, $OD_{bf}(\lambda)$ is the optical density of a fully hydrated blank filter, and OD_{null} is a null wavelength residual correction (750 - 850 nm). V_f is the volume of water filtered and A_f is the clearance area of the filter . Absorption by detritus at 440 nm (a_d440 m^{-1}), and by phytoplankton at 676 nm ($a_{ph}676$ m^{-1}), are used in the present study as an index for absorption by detritus, and phytoplankton, respectively.

2.4. Statistical Analysis

A one-way analysis of variance (ANOVA) test was conducted to assess the differences in the mean values of the respective parameters at the sampling stations during different seasons. The correlation coefficient (r) was computed for a_g412 vs. salinity and chlorophyll-*a*.

3. Results

3.1. Physicochemical characteristics of the estuarine and coastal waters of Goa

The spatiotemporal variations in the physicochemical parameters were similar to those observed for these waters in previous studies (Shetye et al. 2007; Kumar et al. 2004; Maya et al. 2011). The SWM plays an important role in the biological, physical, and chemical variations of the studied estuaries. The temperature and salinity variations in the coastal waters and the Mandovi and Zuari estuaries are presented in Table 1. The temperature was observed to be the highest during the SIM and lowest during the NEM. The coastal waters were not sampled during the SWM period due to the rough weather conditions. The temperature increased from the mouth to the upstream of both estuaries, while an inverse trend was observed for salinity. During the SWM, estuarine waters exhibited stratification, with cold, low-salinity water at the surface and warmer, more saline water at greater depths. Temperature inversions were observed in the coastal waters during the NEM. Chlorophyll-*a* was observed to be higher in the estuaries than that in the coastal waters (except during algal blooms during the SIM). In the estuaries and coastal waters, the highest chlorophyll-*a* contents were observed during SIM and NEM, respectively. The lowest chlorophyll-*a* values in both the estuaries and coastal waters were observed during the fall inter-monsoon (FIM) season.

The absorption by detritus and CDOM contributes significantly to the total light absorption in the coastal and estuarine waters of Goa, while absorption by phytoplankton was insignificant during all

the seasons, except during blooms. The detrital fraction (a_d412 m^{-1}) dominates the estuarine waters during the SWM season whereas the CDOM fraction dominates the coastal waters during all the seasons.

3.2. Optical properties of CDOM in the coastal and estuarine waters of Goa

3.2.1. Variability of a_g412, spectral slope and slope ratio in the Mandovi and Zuari estuaries and the adjoining coastal waters

The ranges of the physicochemical and optical data measured in the two estuaries and the coastal waters between 2014 and 2017 are presented in Table 1. We observed seasonal variability in the CDOM absorption in this study. As expected, for estuarine waters, a_g412 was much higher (0.069 - 1.458 m^{-1}) than that in the coastal waters (0.037 - 0.329 m^{-1}) during all seasons (Table 1). Spectral profiles of CDOM variations in the coastal and estuarine waters on a seasonal basis are given in Fig. S1. The magnitudes of the seasonal mean a_g412 exhibited marked differences in the estuarine (one-way ANOVA: $F = 12.034$, $p < 0.001$) and the coastal waters ($F = 3.390$, $p < 0.05$) during the four seasons. CDOM absorption was highest in the Mandovi and Zuari estuaries during the SIM and SWM seasons. Spatially, CDOM absorption increased linearly from the mouth to the upstream of both estuaries during all seasons, suggesting that there was a significant DOM source upstream of the estuaries ($p < 0.05$). In the coastal waters, the highest and lowest CDOM absorption levels were observed during the SIM and NEM seasons (Table 1). The value of a_g412 decreased with increasing salinity, and higher values were observed close to the coast than those observed offshore during SIM and NEM and vice versa during FIM (Fig. 2). Extensive patches of *Trichodesmium* blooms were observed in the coastal waters during SIM. The CDOM absorption spectra of these samples deviated from the normal exponential behavior and exhibited distinct peaks in the UV and blue regions (Fig. S2). CDOM (a_g412) of the rainwater was low (0.022 – 0.577 m^{-1}) as compared to the estuaries (0.227 – 1.458 m^{-1}) whereas $S_{275-295}$ of the rainwater was high (0.02 - 0.035 nm^{-1}) when compared to the surface waters of estuaries during SWM.

Significant seasonal variations in $S_{250-600}$, $S_{275-295}$, and the slope ratio S_R were observed in the coastal ($p < 0.05$) and estuarine waters ($p < 0.001$). In the coastal waters, $S_{250-600}$ was found to be high during the SIM, and low during the FIM season (Table 1). $S_{275-295}$ was highest in the coastal waters during the SIM season, followed by NEM, and was lowest during the FIM season (Fig. 3). S_R increased towards the offshore stations during the SIM and NEM seasons, while high values were observed at the near-shore stations during the FIM season. Large variability in spectral slopes was observed during SIM and NEM in the coastal waters. Values of a_g412 were higher during March compared to

April and May, whereas S values were lower during March compared to the other two months. A similar pattern of variation was observed during NEM with lower values of a_g412 and higher S during November as compared to other months of NEM. In both estuaries, the lowest values of $S_{250-600}$ and $S_{275-295}$ were observed during the SWM with the increase in runoff from the catchments of the estuaries, while higher values were observed during the SIM period. Seasonal variations in $S_{275-295}$ were marginal in the Mandovi Estuary, while large variations were observed in the Zuari Estuary (Table 1). S_R was highest during the SIM season and lowest during the SWM in both estuaries (Fig. 4). $S_{275-295}$ and S_R (indicators of molecular weight) increased towards the mouth of both estuaries from the upstream. Low-molecular-weight DOM was abundant near the mouths of the estuaries, while high-molecular-weight DOM was dominant in the upstream region, indicating the transformation and dilution of riverine DOM during its passage to the adjoining coastal waters (Figs. 3 and 4). CDOM (a_g412) and S ($S_{275-295}$) showed an inverse relationship during SIM and NEM (Fig. 5), while the presence of multiple sources was evident during SWM (Fig. 5)

3.2.2. Variation of a_g412, spectral slopes, $S_{275-295}$, and S_R with salinity

The mixing curves of a_g412 for Mandovi and Zuari estuaries along with the adjoining coastal waters indicated a distinct non-conservative behavior of CDOM (except during FIM) (Fig. 2). A mixing diagram was constructed by joining the high and low-salinity end members, and the values above and below the theoretical dilution line are attributed to sources and sinks, respectively (Stedmon et al. 2003). In this study, the a_g412 values were below the mixing line at very low (< 2) salinities in the Zuari Estuary during the SWM, and at high (> 33) salinities during SIM and NEM in both the estuaries and coastal waters (Fig. 2). However, additions were observed at salinities between 3 and 32, as indicated by the values above the mixing line. During the FIM, conservative mixing of CDOM was observed in the Zuari Estuary while a quasi-conservative mixing was observed in the Mandovi Estuary (Fig. 2).

The spectral slopes and slope ratio ($S_{250-600}$, $S_{275-295}$, and S_R) exhibited a characteristic pattern with salinity, with an almost constant value ($S_{275-295}$ = 0.019 nm^{-1}, S_R = 1.135) within a salinity range of 3 – 31, while a decrease in S and S_R ($S_{275-295}$ = 0.0085 – 0.016 nm^{-1} and S_R = 0.5 – 0.9) was observed upstream of the estuaries (salinity range of 0 – 3) during SWM. However, at remarkably high salinities (>32), S and S_R exhibited a large variability ($S_{275-295}$ = 0.019 – 0.036 nm^{-1} and S_R = 1 – 3) (Fig. 3 and 4). This suggests that there were variations in the quality of CDOM in both the estuaries and the coastal waters ($p < 0.001$). In general $S_{275-295}$ and S_R increased with salinity due to mixing of terrestrial and marine DOM.

4. Discussion

High CDOM absorption (a_g412) was observed during the SIM and SWM seasons in both the Mandovi and Zuari estuaries. However, these two seasons exhibited contrasting characteristics with basically dry weather, high solar irradiance and no discharge in the former, whereas heavy rainfall, high discharge and low solar irradiance in the latter.

4.1. Variations of CDOM optical properties in the Mandovi and Zuari estuaries during the non-monsoon (SIM and NEM) seasons

During the SIM, sea surface temperature and salinity were found to be the highest and tides are the sole driving force for mixing and circulation in these estuaries during the non-monsoon season (Shetye et al. 2007; Manoj and Unnikrishnan 2009). In addition, river discharge in the estuaries is the lowest (Shetye et al. 2007; Manoj and Unnikrishnan 2009). Hence, the contribution of CDOM in the estuaries from riverine inputs would be insignificant in comparison to that during the SWM and FIM seasons, when river discharges were higher. Phytoplankton is a major source of CDOM in coastal and estuarine waters; however, their contributions to the total CDOM may vary on a regional basis. During the SIM, high CDOM absorption in these estuaries could be attributed to *in-situ* production and the degradation of phytoplankton (Zhang et al. 2009; Loginova et al. 2016), as indicated by the good correlation between CDOM absorption and chlorophyll-*a* (Mandovi Estuary r = 0.95; Zuari Estuary r = 0.93; Fig. 6). This was also substantiated by a good correlation between absorption by phytoplankton ($a_{ph}676$) and a_g412 (r = 0.84). The longer residence time of water (~50 days) during non-monsoon seasons (Shetye et al. 2007) would have favored the accumulation of phytoplankton. The inverse relationship observed between CDOM absorption and $S_{275-295}$ in the coastal and estuarine waters also support the autochthonous production (Fig. 5) and accumulation of marine organics in the estuaries. Mangroves are another potential source of CDOM in these estuaries, and they cover a relatively smaller area in the Zuari Estuary (735 ha) than in the Mandovi Estuary (1107 ha) (Shynu et al. 2015). The leachate from mangrove leaves and stems is a significant source of CDOM (Shank et al. 2010). Anthropogenic activities peak during the SIM, which significantly contribute to CDOM. The petroleum hydrocarbons from river transport systems, such as barges, ferryboats, and trawlers, could also form another source of CDOM (Coble 2007; Chiranjeevulu et al. 2014). Sand mining activities in the Mandovi Estuary during non-monsoon seasons disturb the benthic layers, resulting in the release of organic matter, resulting in CDOM production. Domestic and treated municipality sewage is discharged into these estuaries, which could also serve as a source of CDOM (Baker 2001; Coble 2007; Guo et al. 2010).

The slopes ($S_{250-600}$ and $S_{275-295}$) and slope ratio (S_R) were highest during the SIM in both estuaries (Figs. 3 and 4), indicating that CDOM was modified by photochemical transformation (DelVecchio and Blough 2002; Helms et al. 2008; Yamashita et al. 2013). The residence or flushing times of the Mandovi and Zuari estuaries were found to be approximately 50 days during the non-monsoon seasons (Shetye et al. 2007). A longer residence time of water will cause favorable organic matter conditions for prolonged microbial and photochemical degradation and the generation of CDOM (Mari et al. 2007; Peierls et al. 2012). Overall, during the SIM season, CDOM is largely driven by *in-situ* production and anthropogenic processes in both the estuaries of Goa.

During the NEM, the temperature decreases while the salinity gradually increases. Circulation is largely influenced by tides, which is manifested in the distribution patterns of CDOM (Johnson et al. 2001; Kowalczuk et al. 2003). During the NEM, CDOM was probably contributed by autochthonous production in both the estuaries, as indicated by the good correlation between CDOM and chlorophyll-*a* (Mandovi Estuary r = 0.96, Zuari Estuary r = 0.93; Fig. 6), and $a_{ph}676$ (r = 0.81). This was also observed from the inverse relationship of CDOM with S (Fig. 5). Contribution from other sources were also evident during this season as seen from the additions observed during the mixing behavior (Fig. 2d) and also from the lower slopes (0.017 nm^{-1}) of CDOM absorption (a_g412; between 0.2 and 0.4 m^{-1}) in the Mandovi Estuary (Fig. 5d). The sources of CDOM during the SIM and NEM were presumed to be similar. The autochthonous CDOM in both estuaries likely underwent rapid photochemical and microbial degradation, as indicated by the high $S_{250-600}$, $S_{275-295}$, and S_R values.

4.2. **Variations of CDOM optical properties in the Mandovi and Zuari estuaries during the monsoon season**

CDOM was also higher during the SWM in both the estuaries. Mandovi and Zuari are monsoonal estuaries, as their biogeochemistry is mostly controlled by the freshwater influx received during the SWM (Vijith et al. 2009; Vijith and Shetye 2012). During the SWM, strong south-westerly winds bring about heavy rainfall and subsequent river discharge in these estuaries from June to September. The runoff in the Mandovi Estuary (258 $m^3 s^{-1}$) is much higher than that of the Zuari Estuary (147 $m^3 s^{-1}$) (Rao et al. 2015). The discharge rates in the Mandovi and Zuari estuaries during the SWM were 175 and 125 $m^3 s^{-1}$, respectively. The large influx of freshwater from the rivers joining these estuaries decreases the temperature and salinity of estuarine water (Shetye et al. 2007). The rainfall over the Goa region during SWM is substantial at approximately ~ 2200 mm. There is also considerable daily variability in the rainfall patterns, and runoff would be particularly high during the active phase of the SWM. Hence, the high CDOM during the SWM would largely be controlled by rainfall

(freshwater dilution) and subsequent river runoff from the watersheds of the two estuaries (Table 1). A high CDOM during the high inflow of water into the estuaries has also been reported in previous studies (Medeiros et al. 2015 and Aulló-Maestro et al. 2017). $S_{250-600}$, $S_{275-295}$, and S_R were lowest during the SWM season, indicating that the high terrestrial inputs and soil organic matter from the watershed are sources of CDOM (Table 1) (Green and Blough 1994; DelVecchio and Subramaniam 2004).

The watersheds of these estuaries contain mines, agricultural land, and Khazan lands (which are low-lying areas that are fringed with mangroves and are designed as topo-hydro-engineered agro-aquacultural ecosystems). However, the contribution from mangrove leaf litter would be the lowest during this season because of a period of new growth due to the increased supply of nutrients by freshwater inflow (Wafar et al. 1997). Agricultural inputs would be high due to the cultivation of crops and the use of fertilizers (Nikolaou et al. 2008; Fellman et al. 2010; Heinz et al. 2015). The amount of domestic waste received also would be high during the SWM.

The detrital fraction was high and contributed to CDOM production, as indicated by the good correlation between a_d440 and a_g412 ($r = 0.86$). However, the *in-situ* contributions of phytoplankton appear to be insignificant, as indicated by the poor correlation of CDOM with chlorophyll-*a* (Mandovi Estuary $r = 0.25$; Zuari Estuary $r = -0.29$; Fig. 6). Despite the increased nutrients in the estuary from land runoff, increased discharge rates and faster flushing times do not allow for the accumulation of phytoplankton during the SWM (Rennella and Quiros 2006; Peierls et al. 2012). The presence of multiple sources of CDOM in the estuaries was also evident from the wide variation of $S_{275-295}$ with CDOM absorption (Fig. 5b). Absorption was slightly higher in the Zuari Estuary than that in the Mandovi Estuary during the SWM (Fig. 2b). This could be due to the higher runoff, faster flushing, and greater dilution by the larger number of tributaries in the Mandovi Estuary when compared to that of the Zuari Estuary. The drainage basin of Zuari Estuary is largely located in coastal plains whereas the catchment of Mandovi Estuary is largely in elevated and mountainous regions with narrow coastal plain in the downstream. As the Zuari Estuary flows through the coastal plains, CDOM is dominated by highly aromatic soil organic matter. This was indicated by the lower values of $S_{275-295}$ and S_R in the Zuari than those in the Mandovi Estuary, indicating the predominance of DOM with higher molecular weight in the former. Shynu et al. (2015) reported lower particulate organic carbon to particulate nitrogen ratios (8.7 – 10.1) in the Zuari Estuary than those in the Mandovi Estuary (12.2 – 14.6) due to the predominance of soil organic matter during the SWM. In

addition, the detrital fraction was also higher in Zuari Estuary than in Mandovi Estuary during the SWM.

During the SWM, the cloudy sky during most of the day and the high turbidity of the water column would lower the UV-photic zone (Kowalczuk et al. 2003). The $S_{275-295}$ was low during this season indicating a low level of photochemical transformation. The high inputs of DOM, lower residence time, and lower solar irradiance would have hindered photobleaching. Hence, photobleaching is not a major CDOM-removal process during this season. Microbial degradation would be one of the sinks of CDOM as observed by high a_g412 and lower spectral slope, $S_{250-600}$ and $S_{275-295}$. Contrary to the widely accepted notion that terrestrial CDOM is largely resistant to microbial degradation, recent studies have proved the microbial degradation of terrestrial CDOM and potential CO_2 outgassing (Fasching et al. 2014). The a_g412 and $S_{275-295}$ values deviated from the conservative mixing line in the upstream regions with low salinity (Figs. 2b and 3b). The flocculation or sorption of CDOM would have occurred due to the high particle load indicated by the particulate backscatter $b_{bp}700$ and lower salinities during the SWM (Shynu et al. 2012). Hence, the hydrodynamic conditions in the estuaries determine the sources of DOM during the SWM.

The FIM season is characterized by a steady increase in temperature, a decrease in the level of freshwater, and a corresponding increase in salinity. The upstream regions are still influenced by freshwater, and some rainfall was observed during this period. The absorption of CDOM during this period was lowest in the Mandovi Estuary, while higher CDOM was observed in the Zuari Estuary (Table 1). A plausible reason for the low CDOM in the former could be the low production indicated by low chlorophyll-*a*, and poor correlation with CDOM ($r = 0.35$), greater losses, or the formation of a sink of CDOM. The high absorption by CDOM in the Zuari Estuary is likely due to autochthonous sources indicated by the good correlation between CDOM and chlorophyll-*a* ($r = 0.85$) and higher abundance of zooplankton. Studies conducted by other researchers in the Zuari Estuary observed a peak in zooplankton biomass during this season (Gauns et al. 2015; Bardhan et al. 2015). Based on an experimental study, Steingberg et al. (2004) concluded that the fecal pellets and excretion of metabolites by zooplankton or the exudation of mucus and other extracellular secretions result in CDOM production. High solar irradiance, clear skies, and longer residence times during the FIM season might favor photobleaching or the degradation of CDOM, resulting in higher losses. The rapid degradation of photo-labile and terrestrially derived allochthonous carbon could be another reason for the low CDOM; this was also corroborated by the higher values of $S_{250-600}$ and $S_{275-295}$ in the Mandovi Estuary than those in the Zuari Estuary (Fig. 3c). $S_{275-295}$ increased towards the mouth

of the Mandovi Estuary, suggesting a transformation of DOM and the influences of marine organic matter (Fig. 3c). The bacterial population was also found to be higher in the Mandovi Estuary than in the Zuari Estuary (Rodrigues et al. 2011). The respiration and remineralization of organic matter would have resulted in decreased CDOM. All these factors indicate the rapid degradation of allochthonous carbon by photobleaching or microbial degradation at a faster pace in the Mandovi Estuary than in the Zuari Estuary. Towards the upstream of the Mandovi Estuary, the slope values were still lower, indicating that the CDOM was of terrestrial origin. The Zuari Estuary exhibited low and constant $S_{250\text{-}600}$ values with salinity, indicating the influence of fresh CDOM, which is also indicated by the lower $S_{275\text{-}295}$ and S_R values that reflect the predominance of high-molecular-weight DOM (Figs. 3c and 4c).

Overall, CDOM exhibited significant seasonal variations in the Mandovi Estuary, with a four-fold decrease during the FIM and NEM seasons from its level during the SIM and SWM seasons, but such inter-seasonal variations were not observed in the Zuari Estuary.

4.3. **Contribution of CDOM optical properties from rainfall over the Goa region**

Rainwater would be another source of CDOM during the SWM, though its contributions could be marginal in the estuaries. Globally, rainwater deposits 90 and 340 Tg of DOC per year to the sea and land respectively (Willey et al. 2000), which is an important source of organic carbon to the marine and terrestrial environments. Considering this, an attempt was made to study the CDOM in rainwater for this region during the SWM. Rain affects the CDOM of these waters either directly or indirectly. The mean value of rainwater CDOM (0.113 m^{-1}) was 5 times lower than the CDOM absorption in the estuaries (0.570 m^{-1}) during the SWM. The spectral variations of CDOM in rainwater measured for the first time over this region are given in Fig. S1h. CDOM absorption in the rainwater exhibited an increase after a break between rainfalls, which could be attributed to the buildup of aerosols in the atmosphere during the break. The $S_{275\text{-}295}$ value of rainwater increased drastically towards the end of the SWM season. The levels of aerosols (atmospheric fallout of fly ashes with polyaromatic hydrocarbons from ore processing, industrial activities, and motor vehicle exhausts) were found to be high over the Goa region during the SIM season (Suresh et al. 1996; Satheesh and Srinivasan 2002), and rainfall likely transports these aerosols into the estuaries during the SWM. Detailed analysis using fluorescence clearly showed the presence of humic- and protein-like substances in the rainwater samples (Keiber et al., 2006; Fu et al., 2015; Chen et al., 2016; Bao et al., 2018). In addition, Fu et al. (2015) reported that biomass-burning, fossil fuel combustion and primary biological aerosols were the main sources of fluorescent organics in the Arctic region. Goa has a

large area covering agricultural activities and the biomass is generally burnt to prepare the fields for cultivation before the rains. It has also been shown that the mineral dust from the Middle-East finds its way to the Goa region during storms (Ramaswamy et al., 2017). We speculate that all these factors plausibly contribute to the CDOM in rainwater.

Apart from the small contributions of CDOM directly from the rainwater to the estuaries, monsoons indirectly enhance the CDOM of these waters. A significant positive correlation (r = 0.813) was observed between daily average rainfall over the Goa region and CDOM absorption in the study region (Mandovi and Zuari estuaries) (Fig. S3). The increased rainfall will result in a greater runoff from the catchments into the estuaries and coastal waters that flushes terrestrial CDOM, resulting in an increase in CDOM absorption. However, this will significantly influence the availability of light in the water column. The effect of dilution of CDOM by the increase in rainfall was not significant in this study.

4.4. **Seasonal variations of CDOM optical properties in the coastal waters of Goa**

The absorption of CDOM was highest during the SIM season. Solar irradiance, temperature, and salinity were also high during this period. One of the prominent sources of CDOM in the coastal waters was the large *Trichodesmium* bloom observed in the study area; the senescence of the bloom would increase the CDOM pool. The CDOM spectra of *Trichodesmium* bloom samples were unique owing to the peaks in the UV and blue spectral regions. The peaks in the UV range were due to strong absorption by Mycosporine-like amino acids (MAA), and by phycourobilin and phycoerythrobilin in the visible range (Fig. S2). Autochthonous production could be the primary source of CDOM, as indicated by the good correlation between CDOM and chlorophyll-*a* (r = 0.89; Fig. 7), and $a_{ph}676$ (r = 0.82). However, the chlorophyll-*a* concentration during the bloom was very high and hence these points were not considered in Fig. 7. The a_g412 and $S_{275-295}$ relationship (Fig. 5a) also points out to the autochthonous source. The high $S_{275-295}$ and S_R values corresponding to low CDOM absorption values support in-situ production (Fig. 5a). The observed large variability in the spectral slopes ($S_{250-600}$ and $S_{275-295}$) could be explained by the intra seasonal variations in a_g412 and salinity. High a_g412 and low slope during March could be due to the autochthonous production followed by photo-degradation and bacterial utilization of CDOM (Nelson et al. 2004; Fichot and Benner 2012; Yamashita et al. 2013). The increase in $S_{275-295}$ was observed during the latter months of April- May (except bloom) indicating efficient photobleaching. S_R values were highest in the coastal waters during SIM, demonstrating the predominance of low-molecular-weight CDOM (Table 1). CDOM removal by photobleaching and microbial degradation exceeded the high level of

autochthonous production in the coastal waters during the SIM period. Despite high photobleaching during SIM, absorption of light in the coastal waters was dominated mostly by CDOM (50%) followed by detritus (29%) and least by phytoplankton. The temperature in the coastal waters during the FIM season was remarkably high. The influence of freshwater on the coastal waters was still evident during the FIM season owing to the low salinity (Table 1). In addition to the Mandovi and Zuari estuaries, other small rivers flow into the Arabian Sea. The high CDOM absorption during the FIM season was due to the export of terrigenous organic matter from the catchment areas of the rivers and estuaries to the adjoining coastal waters from heavy flushing during SWM. The terrestrial origin of CDOM was indicated by its optical properties, with low $S_{275\text{-}295}$ and S_R values (Figs. 3c and 4c), indicating the predominance of high-molecular-weight DOM. Detritus absorption (a_d440) and a_g412 exhibited a good correlation (r = 0.64), which further supported the contribution of terrigenous DOM to CDOM production during this season. However, the *in-situ* production of CDOM by phytoplankton was insignificant, as indicated by the poor correlation between CDOM and chlorophyll-*a* (r = 0.37; Fig. 7). The removal of CDOM by photodegradation was also insignificant, as indicated by the low values of $S_{275\text{-}295}$ and S_R (Figs. 3c and 4c), despite the availability of sunlight. The terrestrial pool of CDOM from the estuaries was conservatively diluted during its mixing with the adjoining coastal waters (Fig. 2c).

CDOM absorption was the lowest during the NEM, when there was no external input of freshwater to the coastal region, and it decreased offshore. The contribution of CDOM from the estuaries was low during this season. In general, during the NEM, *in-situ* production of CDOM by the degradation of phytoplankton was a major source of CDOM, as indicated by the good correlation between CDOM and chlorophyll-*a* (r = 0.85; Fig. 7) and $a_{ph}676$ (r = 0.69). This was also observed from the a_g412 and $S_{275\text{-}295}$ relationship (Fig. 5d). The transformation of DOM by photochemical degradation was indicated by the high values of $S_{275\text{-}295}$ and S_R with salinity (Figs. 3d and 4d). Large variability in S observed during the NEM was due to low a_g412 and high S values observed during November which could be attributed to the photochemical degradation of terrestrial DOM (Vodacek et al. 1997; Moran et al 2000) received during the SWM.

4.5. **CDOM mixing behavior**

The mixing patterns of the Mandovi and Zuari estuaries varied seasonally, with a prominent non-conservative mixing behavior. A land-to-sea decreasing trend of CDOM was observed during all the seasons indicating a definite terrestrial influence. An apparent loss of CDOM was observed during the period of high freshwater inflow (majorly terrestrially derived) in the Zuari Estuary at a very low

salinity (Fig. 2b). The terrigenous and highly aromatic nature of DOM in this low salinity region was also supported by its typical optical properties with very low $S_{275-295}$ and S_R values (Figs. 3b and 4b). The scattering of particles given by the backscatter b_{bp} 700(m^{-1}) was higher during the SWM, indicating higher amounts of suspended sediments than those during the non-monsoon seasons. Hence, the loss of CDOM could be attributed to the adsorptive removal by suspended sediments and flocculation when the aromatic content and molecular weight of CDOM (S_R) was high (Fig. 4b) (Uher et al. 2001; Asmala et al. 2014). Wachenfeldt and Tranvik (2008) reported that allochthonous DOM (with humic matter as a major constituent) is a precursor for flocculation in the water column of a Swedish boreal lake. The photobleaching of DOM might be insignificant during the SWM, as solar radiation was lowest due to the high cloud cover and high turbidity of the water column. In contrast, the Mandovi Estuary exhibited apparent additions of CDOM, even during the high-inflow period of the SWM (Fig. 2b). A higher number of tributaries join the Mandovi Estuary, and more CDOM could be exported from these tributaries and their watersheds. Different pools of CDOM were also evident from the a_g412 and $S_{275-295}$ relationship (Fig. 5b). In the Mandovi Estuary, removal due to flocculation seems to be insignificant in comparison to the additions of CDOM. During the FIM season, conservative behavior of CDOM was observed in the Zuari Estuary with the strongest correlation with salinity (r = -0.90), while the Mandovi Estuary exhibited quasi-conservative mixing behavior with additions in the mid-stream region (Fig. 2c). This indicates that the terrigenous source of CDOM in the upstream is significantly diluted during its passage through the estuary during the FIM.

Apparent additions of CDOM were observed in both estuaries during the SIM and NEM seasons (Figs. 2a and 2d), when freshwater inflow was insignificant. Similar results were found in previous studies of other estuarine and coastal waters (Doering et al. 1994; Rochelle-Newall and Fisher 2002, Chen et al. 2015). This indicates that there are sources of CDOM other than the inputs received upstream of the estuary. CDOM input from the watersheds was almost negligible during these seasons. *In-situ* production could be a source of CDOM, as indicated by the good correlation of CDOM and chlorophyll-*a* ($r > 0.9$) during the SIM and NEM seasons. The inverse relationship between a_g412 and $S_{275-295}$ observed in this study shows the influence of marine source in the estuary (Figs. 5a and 5d). The maximum deviation from the theoretical mixing line occurs in the mid-salinity areas, close to the urbanized regions. This region also contains large patches of mangroves and is prone to anthropogenic activities, such as pleasure cruises, shipbuilding, treated sewage discharge, and so on. The deviation from the mixing line is greater in the Mandovi Estuary than that in the Zuari Estuary. Furthermore, more anthropogenic activities occur in the Mandovi Estuary. Hence, our study

clearly indicates the presence of a constant source of CDOM in the midstream region of Mandovi Estuary, which was also evident from the values deviating from the a_g412 and $S_{275-295}$ relationship. This was more pronounced during the NEM in the Mandovi Estuary (Fig. 5d). In the coastal waters, most of the a_g412 values fell below the mixing line (Fig. 3a), indicating the removal of CDOM, which can be attributed to photobleaching. This was also observed from the $S_{275-295}$ and S_R values which increased drastically in the coastal waters indicating the transformation of DOM by the process of photobleaching (Figs. 3 and 4). The results obtained support our hypothesis of non-conservative mixing behavior in these estuaries.

5. Conclusion

In this study, the spatiotemporal variability of CDOM in the estuaries and adjoining coastal waters of Goa, India, was explored. *Autochthonous sources*, inputs from mangroves and anthropogenic activities contributed to the high CDOM during the non-monsoon seasons. The *Trichodesmium* bloom acts as a major autochthonous source of CDOM in the coastal waters during the SIM season. Meanwhile, a high influx of terrestrial organic matter from the watersheds of the estuaries resulted in high CDOM during the monsoon season. Rainfall contributed low amounts of CDOM to the estuaries. The environmental forcing of the SWM plays an important role in regulating CDOM by controlling the inflow from the watersheds and the flushing rate in the estuaries. However, tidal circulation significantly controls the spatial distribution of CDOM during the non-monsoon seasons.

Photobleaching was found to be the dominant sink of CDOM during the non-monsoons season, while removal by flocculation and adsorption at low salinities was observed in the estuaries during the SWM. Non-conservative mixing behavior of CDOM was observed in the waters of Goa during all seasons except the FIM, with large additions in the mid-stream regions and removal at low salinities in the estuaries and by photobleaching in the coastal waters. CDOM was found to modulate the spectral quality of underwater light in the coastal and estuarine waters of Goa. In addition to ocean color remote sensing applications, the present study is important to understand the biogeochemical processes in these waters. Given the usefulness of fluorescence excitation emission matrix (EEM) spectroscopy in source identification of CDOM, our ongoing work will focus on tracing the fluorophores, and towards filling the knowledge gap between the DOC and CDOM in these waters.

Acknowledgments

The authors are thankful to the Director, CSIR-National Institute of Oceanography for providing the facilities and support. We also acknowledge other colleagues who have helped in the field and also in preparation of the manuscript. Indian Meteorological Department (IMD) is kindly acknowledged for providing the rainfall data. A. Dias acknowledges CSIR for providing research fellowship. We sincerely thank the Editor, Associate Editor and the anonymous reviewers for their critical review and suggestions to improve the quality of the manuscript. We also acknowledge 'Editage' for their assistance in language correction. This work was carried out under MOP-3 project funded by Space Application Centre (Indian Space Research Organization), Ahmedabad, India. This is NIO contribution no. xxxx.

References

Asmala, E., D. G. Bowers, R. Autio, H. Kaartokallio, and D. N. Thomas. 2014. Qualitative changes of riverine dissolved organic matter at low salinities due to flocculation. *Journal of Geophysical Research: Biogeosciences*, 119(10), 1919-1933.

Aulló-Maestro, M. E., P. Hunter, E. Spyrakos, P. Mercatoris, A. W. Kovacs, H. Horváth, T. Preston, M. Présing, J. T. Palenzuela, and A. Tyler. 2017. Spatio-seasonal variability of chromophoric dissolved organic matter absorption and responses to photobleaching in a large shallow temperate lake. *Biogeosciences*, 14(5), 1215.

Baker, A. 2001. Fluorescence excitation− emission matrix characterization of some sewage-impacted rivers. *Environmental science & technology*, 35(5), 948-953.

Bao, H., Y. Yi, C. Wang, R. G.Spencer, X. Deng, & W. Guo. 2018. Dissolved organic matter in coastal rainwater: Concentration, bioavailability and depositional flux to seawater in southeastern China. *Marine Chemistry*, *205*, 48-55.

Bardhan, P., S. G. Karapurkar, D. M. Shenoy, S. Kurian, A. Sarkar, M. V. Maya, H. Naik, S. Varik, and S. W. A. Naqvi. 2015. Carbon and nitrogen isotopic composition of suspended particulate organic matter in Zuari Estuary, west coast of India. *Journal of Marine Systems*, 141, 90-97.

Battin, T. J., S. Luyssaert, L. A. Kaplan, A. K. Aufdenkampe, A. Richter, and L. J. Tranvik. 2009. The boundless carbon cycle. *Nature Geoscience*, 2(9), 598.

Blough, N. V., and S. A. Green. 1995. Spectroscopic characterization and remote sensing of non-living organic matter. *The Role of Non-living Organic Matter in the Earth's Carbon Cycle (RG Zepp and C. Sonntag, eds.), John Wiley & Sons Ltd*, 23-45.

Carder, K. L., S. K. Hawes, K. A. Baker, R. C. Smith, R. G. Steward, and B. G. Mitchell. 1991. Reflectance model for quantifying chlorophyll *a* in the presence of productivity degradation products. Journal of Geophysical Research: Oceans, 96(C11), 20599-20611.

Carder, K. L., R. G. Steward, G. R. Harvey, and P. B. Ortner. 1989. Marine humic and fulvic acids: Their effects on remote sensing of ocean chlorophyll. *Limnology and oceanography*, 34(1), 68-81.

Chen, Z., P. H. Doering, M. Ashton, and B. A. Orlando. 2015. Mixing behavior of colored dissolved organic matter and its potential ecological implication in the Caloosahatchee River estuary, Florida. *Estuaries and coasts*, 38(5), 1706-1718.

Chiranjeevulu, G., K. N. Murty, N. S. Sarma, R. Kiran, N. V. H. K. Chari, S. R. Pandi, P. Venkatesh, C. Annapurna, and K. N. Rao. 2014. Colored dissolved organic matter signature and phytoplankton response in a coastal ecosystem during mesoscale cyclonic (cold core) eddy. *Marine environmental research*, 98, 49-59.

Chen, Q., Miyazaki, Y., Kawamura, K., Matsumoto, K., Coburn, S., Volkamer, R., ... & Ramasamy, S. (2016). Characterization of chromophoric water-soluble organic matter in urban, forest, and marine aerosols by HR-ToF-AMS analysis and excitation–emission matrix spectroscopy. *Environmental science & technology*, *50*(19), 10351-10360.

Coble, P. G. 2007.Marine optical biogeochemistry: the chemistry of ocean color. *Chemical reviews*, 107(2), 402-418.

DeGrandpre, M. D., A. Vodacek, R. K. Nelson, E. J. Bruce, and N. V. Blough. 1996. Seasonal seawater optical properties of the US Middle Atlantic Bight. *Journal of Geophysical Research: Oceans*, 101(C10), 22727-22736.

Del Vecchio, R., and A. Subramaniam. 2004. Influence of the Amazon River on the surface optical properties of the western tropical North Atlantic Ocean. *Journal of Geophysical Research: Oceans*, 109(C11).

Del Vecchio, R., and N. V. Blough. 2002. Photobleaching of chromophoric dissolved organic matter in natural waters: kinetics and modeling. *Marine Chemistry*, 78(4), 231-253.

Desa, E. S., T. Suresh, , S. G. P. Matondkar, E. Desa, J. Goes, A. A. M. Q. Mascarenhas,... & C. E. G. Fernandes. 2005. Detection of Trichodesmium bloom patches along the eastern Arabian Sea by IRS-P4/OCM ocean color sensor and by in-situ measurements. *Journal of Geo-Marine Sciences,*34(4), 374-386.

Dias, A. B., T. Suresh, A. Sahay, and P. Chauhan. 2017. Contrasting characteristics of colored dissolved organic matter of the coastal and estuarine waters of Goa during summer. *Indian journal of geo-marine sciences,* 46(05), 860-870.

Doering, P. H., C. A. Oviatt, J. H. McKenna, and L. W. Reed. 1994. Mixing behavior of dissolved organic carbon and its potential biological significance in the Pawcatuck River Estuary. *Estuaries*, 17(3), 521-536.

Fasching, C., Behounek, B., Singer, G. A., & Battin, T. J. (2014). Microbial degradation of terrigenous dissolved organic matter and potential consequences for carbon cycling in brown-water streams. *Scientific reports*, *4*, 4981.

Fellman, J. B., E. Hood, and R. G.M. Spencer. 2010. Fluorescence spectroscopy opens new windows into dissolved organic matter dynamics in freshwater ecosystems: A review. *Limnology and Oceanography*, 55(6), 2452-2462.

Fichot, C. G., and R. Benner. 2012. The spectral slope coefficient of chromophoric dissolved organic matter (S275–295) as a tracer of terrigenous dissolved organic carbon in river□influenced ocean margins. *Limnology and Oceanography*, *57*(5), 1453-1466.

Fu, P., Kawamura, K., Chen, J., Qin, M., Ren, L., Sun, Y., ... & Yamashita, Y. (2015). Fluorescent water-soluble organic aerosols in the High Arctic atmosphere. *Scientific reports*, *5*, 9845.

Gauns, M., S. Mochemadkar, S. Patil, A. Pratihary, S. W. A. Naqvi, and M. Madhupratap. 2015. Seasonal variations in abundance, biomass and grazing rates of microzooplankton in a tropical monsoonal estuary. *Journal of oceanography*, 71(4), 345-359.

Gomes, H., J. I. Goes, S.G. P. Matondkar, S. G. Parab, A. R.N. Al-Azri, and P. G. Thoppil. 2008. Blooms of Noctiluca miliaris in the Arabian Sea—An in situ and satellite study. *Deep Sea Research Part I: Oceanographic Research Papers*, 55(6), 751-765.

Gonsalves, M. J., S. Nair, P.A. Loka Bharathi, and D. Chandramohan. 2009. Abundance and production of particle-associated bacteria and their role in a mangrove-dominated estuary. *Aquatic Microbial Ecology,* 57(2), 151-159.

Green, S. A., and N. V. Blough. 1994. Optical absorption and fluorescence properties of chromophoric dissolved organic matter in natural waters. *Limnology and Oceanography*, 39(8), 1903-1916.

Groom, S. B., S. Sathyendranath, Y. Ban, S. Bernard, B. Brewin, V. Brotas, ... & S. Ciavatta. 2019. Satellite ocean colour: current status and future perspective. *Frontiers in Marine Science*, *6*(485), 1-30.

Guo, W., J. Xu, J. Wang, Y. Wen, J. Zhuo, and Y. Yan. 2010. Characterization of dissolved organic matter in urban sewage using excitation emission matrix fluorescence spectroscopy and parallel factor analysis. *Journal of Environmental Sciences*, 22(11), 1728-1734.

Heinz, M., D. Graeber, D. Zak, E. Zwirnmann, J. Gelbrecht, and M. T. Pusch. 2015. Comparison of organic matter composition in agricultural versus forest affected headwaters with special emphasis on organic nitrogen. *Environmental science & technology*, 49(4), 2081-2090.

Helms, J. R., A. Stubbins, J. D. Ritchie, E. C. Minor, D. J. Kieber, and K. Mopper. 2008. Absorption spectral slopes and slope ratios as indicators of molecular weight, source, and photobleaching of chromophoric dissolved organic matter. *Limnology and Oceanography*, 53(3), 955-969.

Jerlov, N. G., 1976. Marine optics, *Elsevier Oceanography Series* 14.

Johnson, D. R., A. Weidemann, R. Arnone, and C. O. Davis. 2001. Chesapeake Bay outflow plume and coastal upwelling events: physical and optical properties. *Journal of Geophysical Research: Oceans*, 106(C6), 11613-11622.

Kieber, R. J., R. F. Whitehead, S. N. Reid, D. Joan. 2006. Chromophoric dissolved organic matter (CDOM) in rainwater, southeastern North Carolina, USA. *Journal of Atmospheric Chemistry,* 54(1), 21-41.

Knap, A. H., A. Michaels, A. R. Close, H. Ducklow, and A. G. Dickson. 1996. Protocols for the joint global ocean flux study (JGOFS) core measurements.

Kowalczuk, P., Stoń-Egiert, J., Cooper, W.J., Whitehead, R.F. and Durako, M.J., 2005. Characterization of chromophoric dissolved organic matter (CDOM) in the Baltic Sea by excitation emission matrix fluorescence spectroscopy. *Marine Chemistry*, *96*(3-4), pp.273-292.

Kowalczuk, P., W. J. Cooper, R. F. Whitehead, M. J. Durako, and W. Sheldon. 2003. Characterization of CDOM in an organic-rich river and surrounding coastal ocean in the South Atlantic Bight. *Aquatic Sciences-Research Across Boundaries*, 65(4), 384-401.

Krishnakumari, L., P. M. A. Bhattathiri, S. G. P. Matondkar, and J. John. 2002. Primary productivity in Mandovi-Zuari estuaries in Goa. *J. Mar. Biol. Ass. India*, 44, 1–13.

Kumar, P. S., J. Narvekar, A. Kumar, C. Shaji, P. Anand, P. Sabu, G. Rijomon et al. 2004. Intrusion of the Bay of Bengal water into the Arabian Sea during winter monsoon and associated chemical and biological response. *Geophysical Research Letters*, 31(15).

Loginova, A. N., S. Thomsen, and A. Engel. 2016. Chromophoric and fluorescent dissolved organic matter in and above the oxygen minimum zone off Peru. *Journal of Geophysical Research: Oceans*, 121(11), 7973-7990.

Loiselle, S., D. Vione, C. Minero, V. Maurino, A. Tognazzi, A. M. Dattilo, C. Rossi, and L. Bracchini. 2012. Chemical and optical phototransformation of dissolved organic matter. Water research, 46(10), 3197-3207.

Manoj, N. T., and A. S. Unnikrishnan. 2009. Tidal circulation and salinity distribution in the Mandovi and Zuari estuaries: case study. *Journal of waterway, port, coastal, and ocean engineering,* 135(6), 278-287.

Mari, X., E. Rochelle-Newall, J. P. Torréton, O. Pringault, A. Jouon, and C. Migon. 2007. Water residence time: a regulatory factor of the DOM to POM transfer efficiency. *Limnology and Oceanography*, 52(2), 808-819.

Maya, M. V., S. G. Karapurkar, H. Naik, R. Roy, D. M. Shenoy, and S. W. A. Naqvi. 2011. Intra-annual variability of carbon and nitrogen stable isotopes in suspended organic matter in waters of the western continental shelf of India. *Biogeosciences*, 8, 3441-3456.

Medeiros, P. M., M. Seidel, T. Dittmar, W. B. Whitman, and M. A. Moran. 2015. Drought-induced variability in dissolved organic matter composition in a marsh-dominated estuary. *Geophysical Research Letters*, 42(15), 6446-6453.

Menon, H. B., N. P. Sangekar, A. A. Lotliker, and P. Vethamony. 2011. Dynamics of chromophoric dissolved organic matter in Mandovi and Zuari estuaries—A study through in situ and satellite data. *ISPRS journal of photogrammetry and remote sensing*, 66(4), 545-552.

Mitchell, B. G., Kahru, M., Wieland, J., Stramska, M., & Mueller, J. L. (2002). Determination of spectral absorption coefficients of particles, dissolved material and phytoplankton for discrete water samples. *Ocean optics protocols for satellite ocean color sensor validation, Revision*, *3*(2), 231.

Moran, M. A., Sheldon Jr, W. M., & Zepp, R. G. (2000). Carbon loss and optical property changes during long□term photochemical and biological degradation of estuarine dissolved organic matter. *Limnology and Oceanography*, *45*(6), 1254-1264.

Mueller, J. L., G. S. Fargion, C. R. McClain, S. Pegau, J. R. V. Zanefeld, B. Gregg Mitchell, M. Kahru, J. Wieland, and M. Stramska. 2003. Ocean optics protocols for satellite ocean color sensor validation, revision 4, volume IV: Inherent optical properties: Instruments, characterizations, field measurements and data analysis protocols.

Naqvi, S. W. A., H. Naik, A. Jayakumar, A. K. Pratihary, G. Narvenkar, S. Kurian, R. Agnihotri, M. S. Shailaja, and P. V. Narvekar. 2009. Seasonal anoxia over the western Indian continental shelf. *Indian Ocean Biogeochemical Processes and Ecological Variability*, 1, 333-345.

Naqvi, S. W. A., H. Naik, A. Jayakumar, M. S. Shailaja, & P. V. Narvekar. 2006. Seasonal oxygen deficiency over the western continental shelf of India. In Past and present water column anoxia (pp. 195-224). Springer Netherlands.

Naqvi, S. W. A., H. Naik, D. A. Jayakumar, M. S. Shailaja, and P. V. Narvekar. 2000. Increased marine production of N2O due to intensifying anoxia on the Indian continental shelf. *Nature,* 408(6810), 346.

Naqvi, S. W. A., M. D. George, P. V. Narvekar, D. A. Jayakumar, M. S. Shailaja, S. Sardessai, V. V. S. S. Sarma et al. 1998. Severe fish mortality associated with 'redtide' observed in the sea off Cochin.

Nelson, N. B., and D. A. Siegel. 2013. The global distribution and dynamics of chromophoric dissolved organic matter. *Annual Review of Marine Science*, 5, 447-476.

Nelson, N. B., C. A. Carlson, and D. K. Steinberg. 2004. Production of chromophoric dissolved organic matter by Sargasso Sea microbes. *Marine Chemistry*, 89(1), 273-287.

Nikolaou, A. D., S. Meric, D. F. Lekkas, V. Naddeo, V. Belgiorno, S. Groudev, and A. Tanik. 2008. Multi-parametric water quality monitoring approach according to the WFD application in Evros trans-boundary river basin: priority pollutants. *Desalination*, 226(1), 306-320.

Para, J., Coble, P., Charrière, B., Tedetti, M., Fontana, C. and Sempere, R., 2010. Fluorescence and absorption properties of chromophoric dissolved organic matter (CDOM) in coastal surface waters of the northwestern Mediterranean Sea, influence of the Rhône River. *Biogeosciences*, *7*(12), pp.4083-4103.

Pednekar, S. M., S. G. P. Matondkar, and V. Kerkar. 2012. Spatiotemporal distribution of harmful algal flora in the tropical estuarine complex of Goa, India. *The Scientific World Journal*, 1-11.

Peierls, B. L., N. S. Hall, and H. W. Paerl. 2012. Non-monotonic responses of phytoplankton biomass accumulation to hydrologic variability: a comparison of two coastal plain North Carolina estuaries. *Estuaries and coasts*, 35(6), 1376-1392.

Ramaswamy, V., P. M. Muraleedharan, & C. P. Babu. 2017. Mid-troposphere transport of Middle-East dust over the Arabian Sea and its effect on rainwater composition and sensitive ecosystems over India. *Scientific reports*, *7*(1), 1-8.

Rao, V. P., R. Shynu, S. K. Singh, S. W. A. Naqvi, and P. M. Kessarkar. 2015. Mineralogy and Sr–Nd isotopes of SPM and sediment from the Mandovi and Zuari estuaries: Influence of weathering and anthropogenic contribution. *Estuarine, Coastal and Shelf Science*, 156, 103-115.

Rennella, A. M., and R. Quiros. 2006.The effects of hydrology on plankton biomass in shallow lakes of the Pampa Plain. *Hydrobiologia*, 556(1), 181-191.

Rochelle-Newall, E. J., and T. R. Fisher. 2002.Chromophoric dissolved organic matter and dissolved organic carbon in Chesapeake Bay. *Marine Chemistry*, 77(1), 23-41.

Rodrigues, V., N. Ramaiah, S. Kakti, and D. Samant. 2011. Long-term variations in abundance and distribution of sewage pollution indicator and human pathogenic bacteria along the central west coast of India. *Ecological indicators*, 11(2), 318-327.

Satheesh, S. K., & Srinivasan, J. (2002). Enhanced aerosol loading over Arabian Sea during the pre□monsoon season: Natural or anthropogenic?. *Geophysical Research Letters*, *29*(18), 21-1.

Shank, G. C., Zepp, R. G., Vähätalo, A., Lee, R., & Bartels, E. (2010). Photobleaching kinetics of chromophoric dissolved organic matter derived from mangrove leaf litter and floating Sargassum colonies. *Marine Chemistry*, *119*(1-4), 162-171.

Shetye, S. R., M. D. Kumar, and D. Shankar. 2007. The Mandovi and Zuari Estuaries.

Shynu, R., V. P. Rao, V. V. S. S. Sarma, P. M. Kessarkar, and R. M. Murali. 2015. Sources and fate of organic matter in suspended and bottom sediments of the Mandovi and Zuari estuaries, western India. *Current science,* 108(2), 226-238.

Shynu, R., V. P. Rao, P. M. Kessarkar, and T. G. Rao. 2012. Temporal and spatial variability of trace metals in suspended matter of the Mandovi estuary, central west coast of India. *Environmental Earth Sciences*, 65(3), 725-739.

Stedmon, C. A., S. Markager, and R. Bro. 2003. Tracing dissolved organic matter in aquatic environments using a new approach to fluorescence spectroscopy. *Marine Chemistry*, 82(3), 239-254.

Steinberg, D. K., N. B. Nelson, C. A. Carlson, and A. Prusak. 2004. Production of chromophoric dissolved organic matter (CDOM) in the open ocean by zooplankton and the colonial cyanobacterium Trichodesmium spp. *Marine Ecology Progress Series*, 267, 45-56.

Suresh, T., E. Desa, , R. G. P. Desai, A. Jayaraman, , & P. Mehra. 1996. Photosynthetically available radiation in the central and eastern Arabian Sea. *Current Science*, 71(11), 883.

Twardowski, M. S., E. Boss, J. M. Sullivan, and P. L. Donaghay. 2004. Modeling the spectral shape of absorption by chromophoric dissolved organic matter. *Marine Chemistry*, 89(1), 69-88.

Uher, G., C. Hughes, G. Henry, and R. C. Upstill-Goddard. 2001. Non-conservative mixing behavior of colored dissolved organic matter in a humic-rich, turbid estuary. *Geophysical Research Letters*, 28(17), 3309-3312.

Vantrepotte, V., Danhiez, F.P., Loisel, H., Ouillon, S., Mériaux, X., Cauvin, A. and Dessailly, D., 2015. CDOM-DOC relationship in contrasted coastal waters: implication for DOC retrieval from ocean color remote sensing observation. *Optics express*, *23*(1), pp.33-54.

Vijith, V., and S. R. Shetye. 2012. A stratification prediction diagram from characteristics of geometry, tides and runoff for estuaries with a prominent channel. *Estuarine, Coastal and Shelf Science*, 98, 101-107.

Vijith, V., D. Sundar, and S. R. Shetye. 2009.Time-dependence of salinity in monsoonal estuaries. *Estuarine, Coastal and Shelf Science*, 85(4), 601-608.

Vodacek, A., Blough, N. V., DeGrandpre, M. D., DeGrandpre, M. D., & Nelson, R. K. (1997). Seasonal variation of CDOM and DOC in the Middle Atlantic Bight: Terrestrial inputs and photooxidation. *Limnology and Oceanography*, *42*(4), 674-686.

Vodacek, A., S. A. Green, and N. V. Blough. 1994. An experimental model of the solar-stimulated fluorescence of chromophoric dissolved organic matter. *Limnology and oceanography*, 39(1), 1-11.

Wachenfeldt, E., and L. J. Tranvik. 2008. Sedimentation in boreal lakes—the role of flocculation of allochthonous dissolved organic matter in the water column. *Ecosystems*, 11(5), 803-814.

Wafar, S., A. G. Untawale, and M. Wafar. 1997. Litter fall and energy flux in a mangrove ecosystem. *Estuarine, Coastal and Shelf Science*, 44(1), 111-124.

Willey, J. D., R. J. Kieber, M. S. Eyman, & G. B. Avery Jr. 2000. Rainwater dissolved organic carbon: concentrations and global flux. *Global Biogeochemical Cycles*, *14*(1), 139-148.

Yamashita, Y., Y. Nosaka, K. Suzuki, H. Ogawa, K. Takahashi, and H. Saito. 2013. Photobleaching as a factor controlling spectral characteristics of chromophoric dissolved organic matter in open ocean. *Biogeosciences*, 10(11), 7207-7217.

Yamashita, Y. and Tanoue, E., 2009. Basin scale distribution of chromophoric dissolved organic matter in the Pacific Ocean. *Limnology and Oceanography*, *54*(2), pp.598-609.

Zhang, Y., M. A. van Dijk, M. Liu, G. Zhu, and B. Qin. 2009. The contribution of phytoplankton degradation to chromophoric dissolved organic matter (CDOM) in eutrophic shallow lakes: field and experimental evidence. *water research*, 43(18), 4685-4697.

Figure Captions

Figure 1: The study area indicating the sampling stations in the coastal waters of Goa and in the Mandovi and Zuari estuaries. It also depicts the anthropogenic activities occurring in the estuaries of Goa.

Figure 2. The conservative mixing diagram showing the variations of a_g412 (m^{-1}) with salinity in the Mandovi and Zuari estuaries, and the adjoining coastal waters. The black continuous line represents the theoretical dilution line (joins the lowest and highest salinity end members) for Zuari and the dotted line represents the Mandovi Estuary. The red continuous line represents the linear fit for Zuari and the dotted line represents the Mandovi Estuary.

Figure 3: Variation of $S_{275-295}$ (nm^{-1}) with salinity in the Mandovi and Zuari estuaries, and the adjoining coastal waters. The black discontinuous line represents the nonlinear fit for Mandovi and the continuous line for Zuari Estuary.

Figure 4: Variation of S_R with salinity in the Mandovi and Zuari estuaries, and the adjoining coastal waters. The black discontinuous line represents the nonlinear fit for Mandovi and the continuous line for Zuari Estuary.

Figure 5: Variation of a_g412 (m^{-1}) with $S_{275-295}$ (nm^{-1}) in the estuaries and the adjoining coastal waters.

Figure 6: Correlation between CDOM absorption (a_g412) and chlorophyll-*a* during the SIM, SWM, FIM and NEM in the Mandovi (red) and Zuari (blue) estuaries.

Figure 7: Correlation between CDOM absorption (a_g412) and chlorophyll-*a* during the SIM, FIM and NEM in the coastal waters. Please note that the chlorophyll-*a* concentration during *Trichodesmium* bloom was very high and hence these points were not considered.

Figure 1

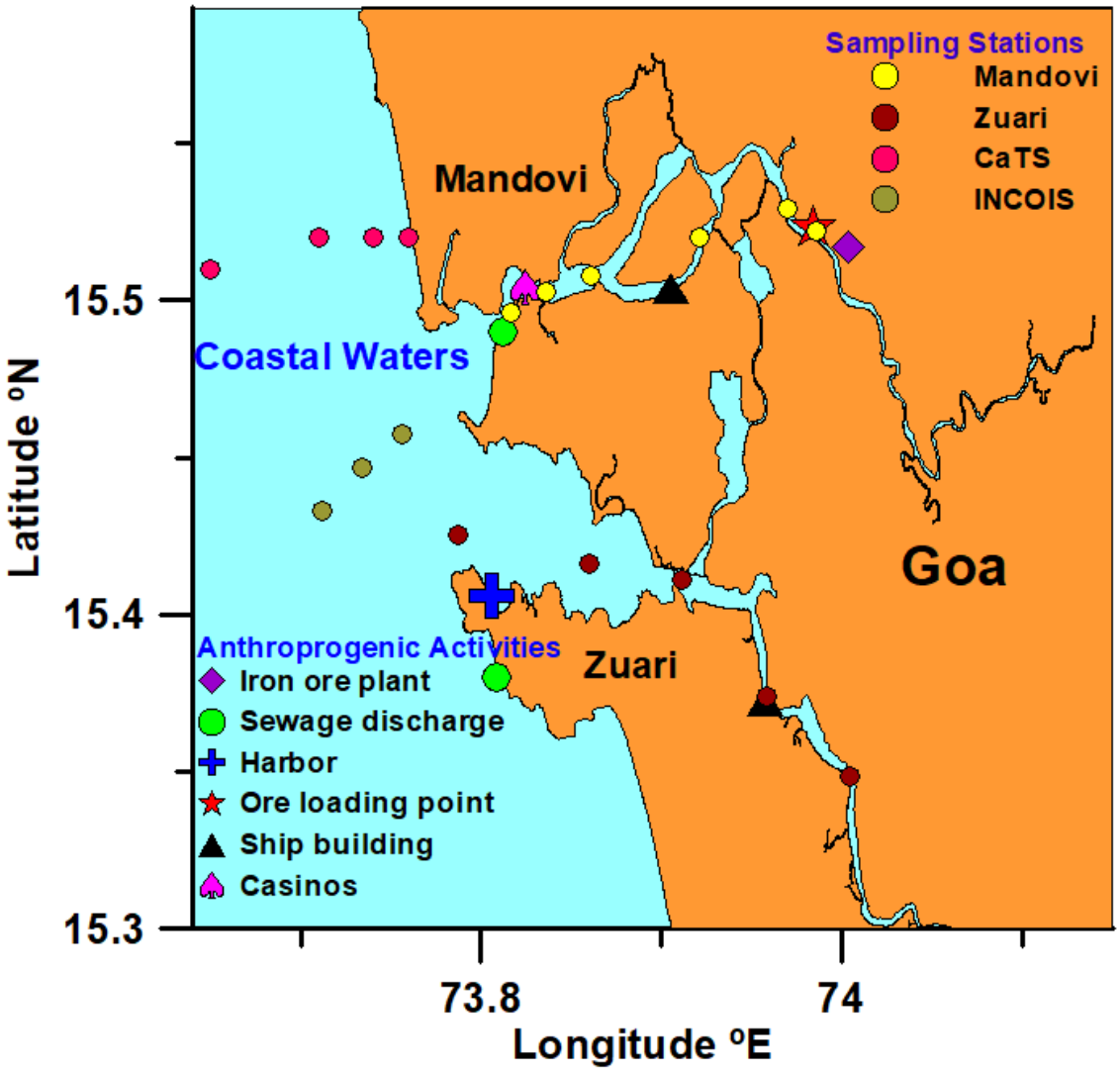
Sampling Stations
Mandovi
Zuari
CaTS
INCOIS
Mandovi
Coastal Waters
Goa
Zuari
Anthroprogenic Activities
Iron ore plant
Sewage discharge
Harbor
Ore loading point
Ship building
Casinos
15.5
15.4
15.3
Latitude °N
73.8
74
Longitude °E

Figure 2

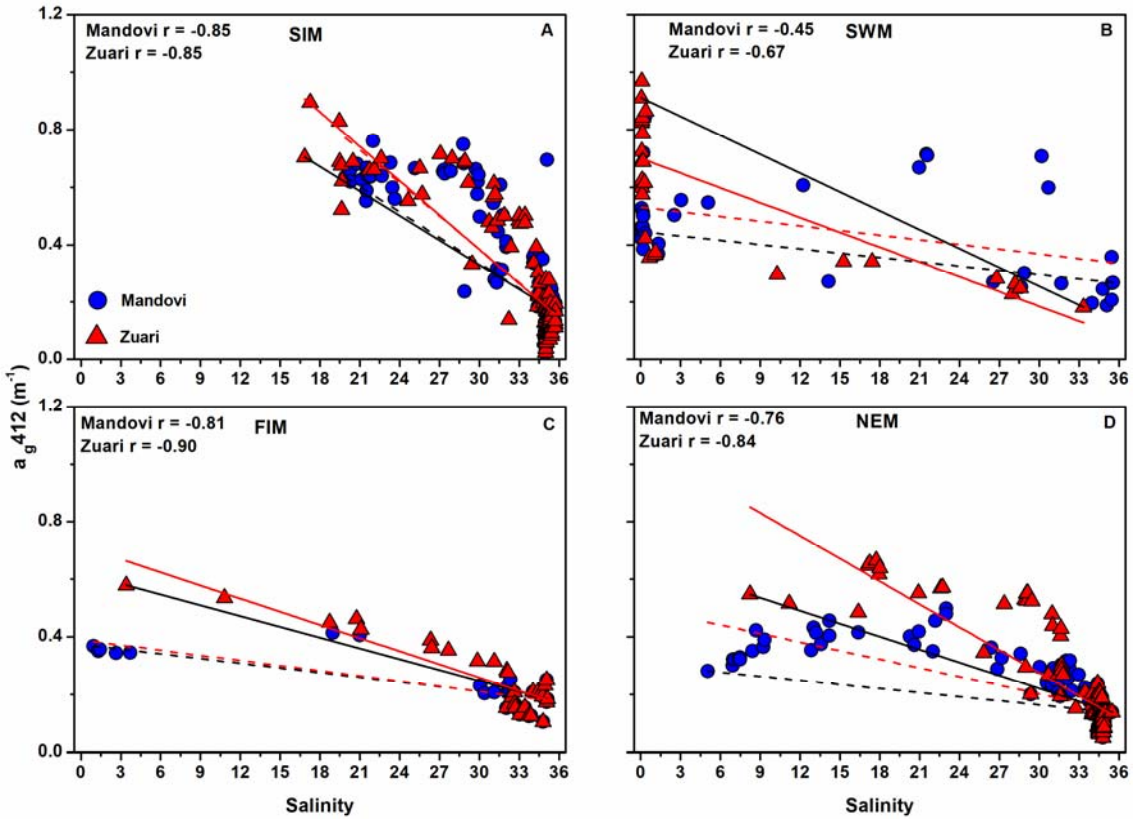
Mandovi r = -0.85
Zuari r = -0.85
SIM
A
Mandovi
Zuari
Mandovi r = -0.45
Zuari r = -0.67
SWM
B
Mandovi r = -0.81
Zuari r = -0.90
FIM
C
Mandovi r = -0.76
Zuari r = -0.84
NEM
D
a g 412 (m-1)
Salinity
Salinity

Figure 3

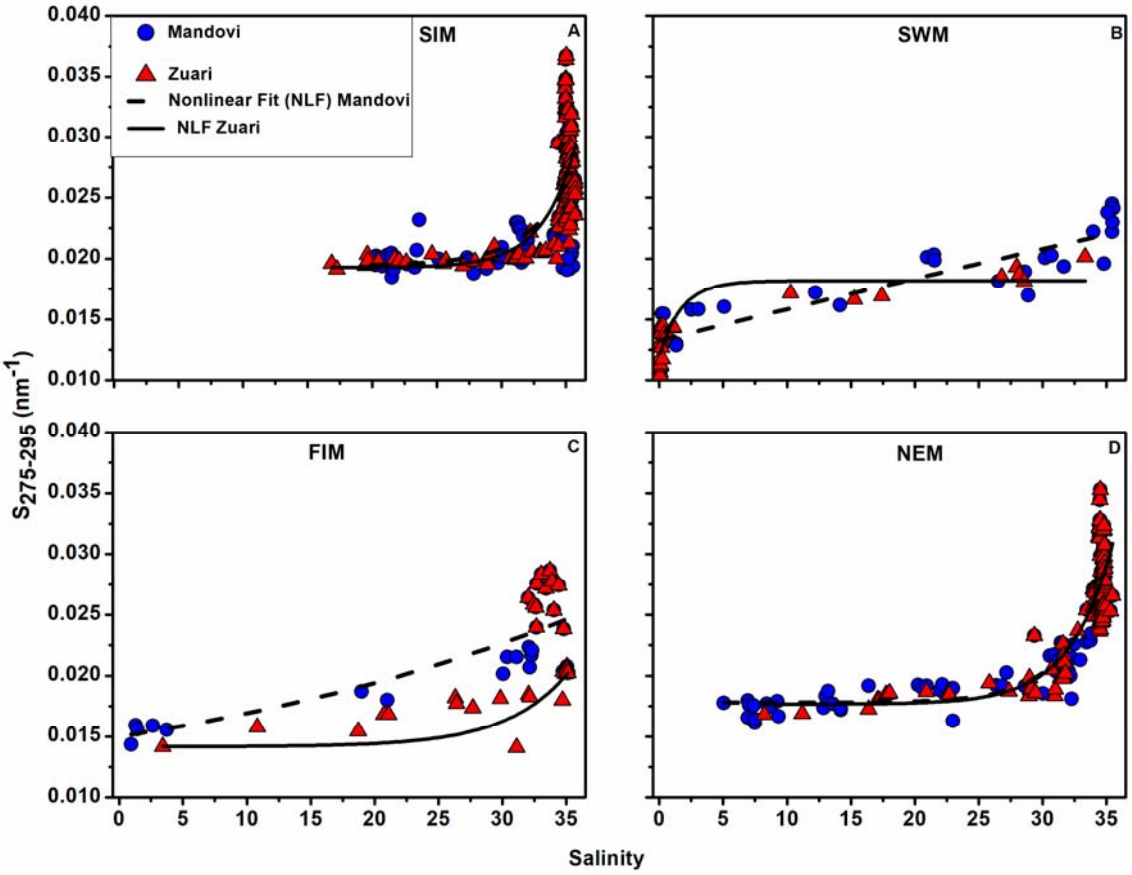
Mandovi
Zuari
Nonlinear Fit (NLF) Mandovi
NLF Zuari
SIM
A
SWM
B
FIM
C
NEM
D
$S_{275-295}$ (nm^{-1})
Salinity
0.040
0.035
0.030
0.025
0.020
0.015
0.010
0
5
10
15
20
25
30
35

Figure 4

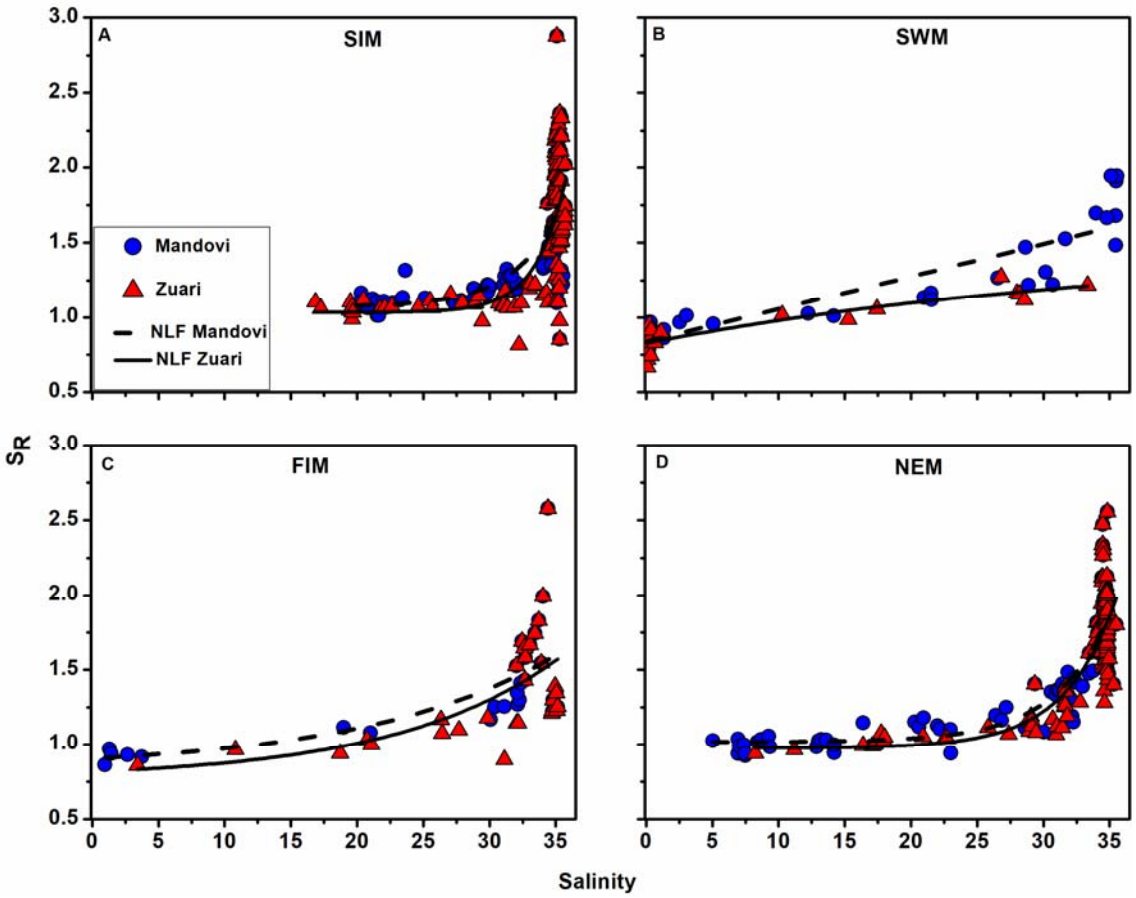
A
SIM
B
SWM
C
FIM
D
NEM
Mandovi
Zuari
NLF Mandovi
NLF Zuari
S_R
Salinity
3.0
2.5
2.0
1.5
1.0
0.5
0
5
10
15
20
25
30
35

Figure 5

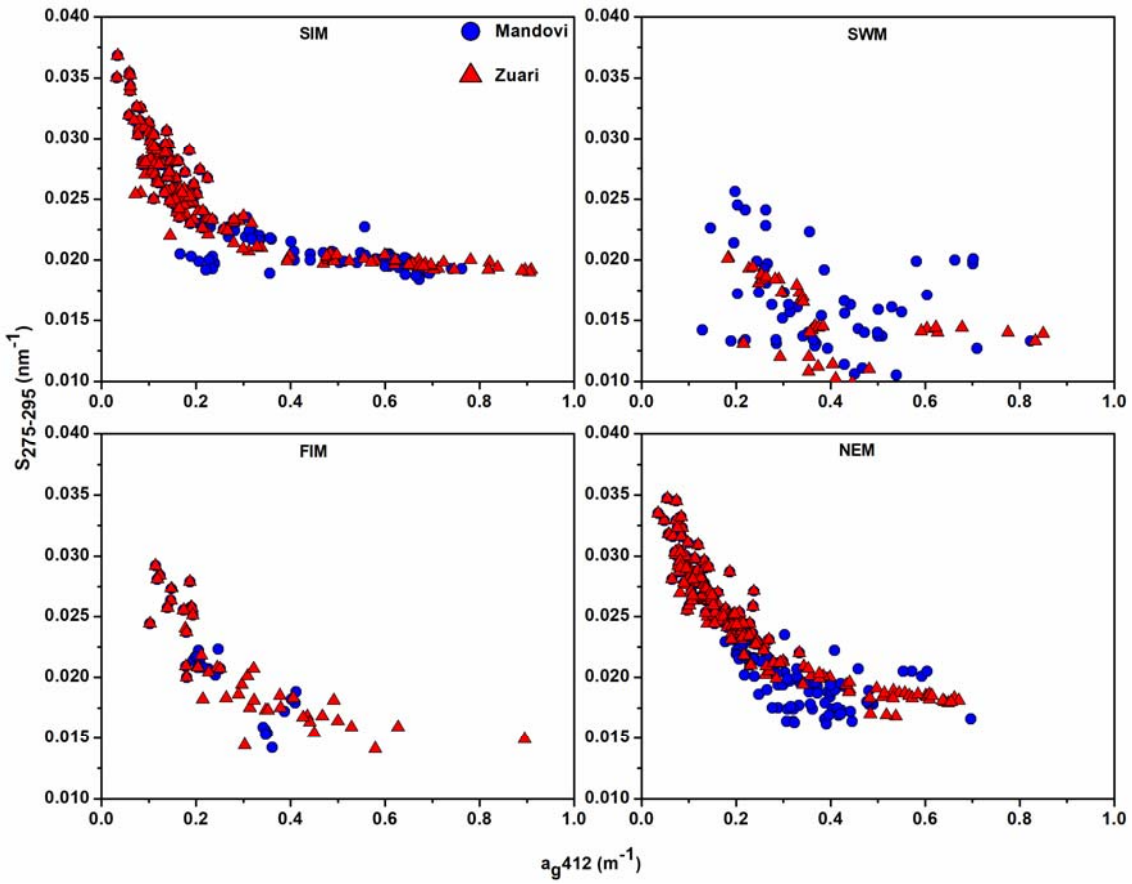
SIM
Mandovi
Zuari
SWM
FIM
NEM
$S_{275-295}$ (nm^{-1})
a_g412 (m^{-1})
0.040
0.035
0.030
0.025
0.020
0.015
0.010
0.0
0.2
0.4
0.6
0.8
1.0

Figure 6

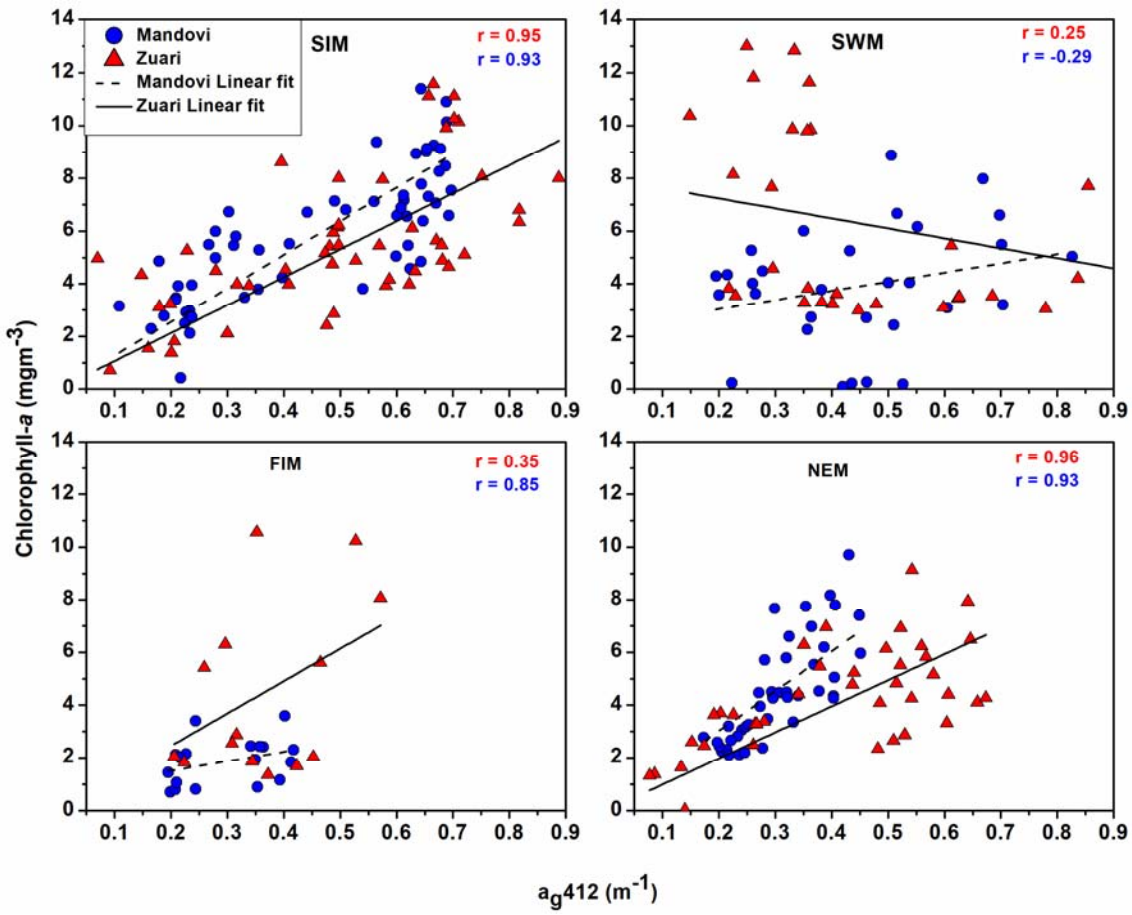
Mandovi
Zuari
Mandovi Linear fit
Zuari Linear fit
SIM
r = 0.95
r = 0.93
SWM
r = 0.25
r = -0.29
FIM
r = 0.35
r = 0.85
NEM
r = 0.96
r = 0.93
Chlorophyll-a (mgm-3)
ag412 (m-1)

Figure 7

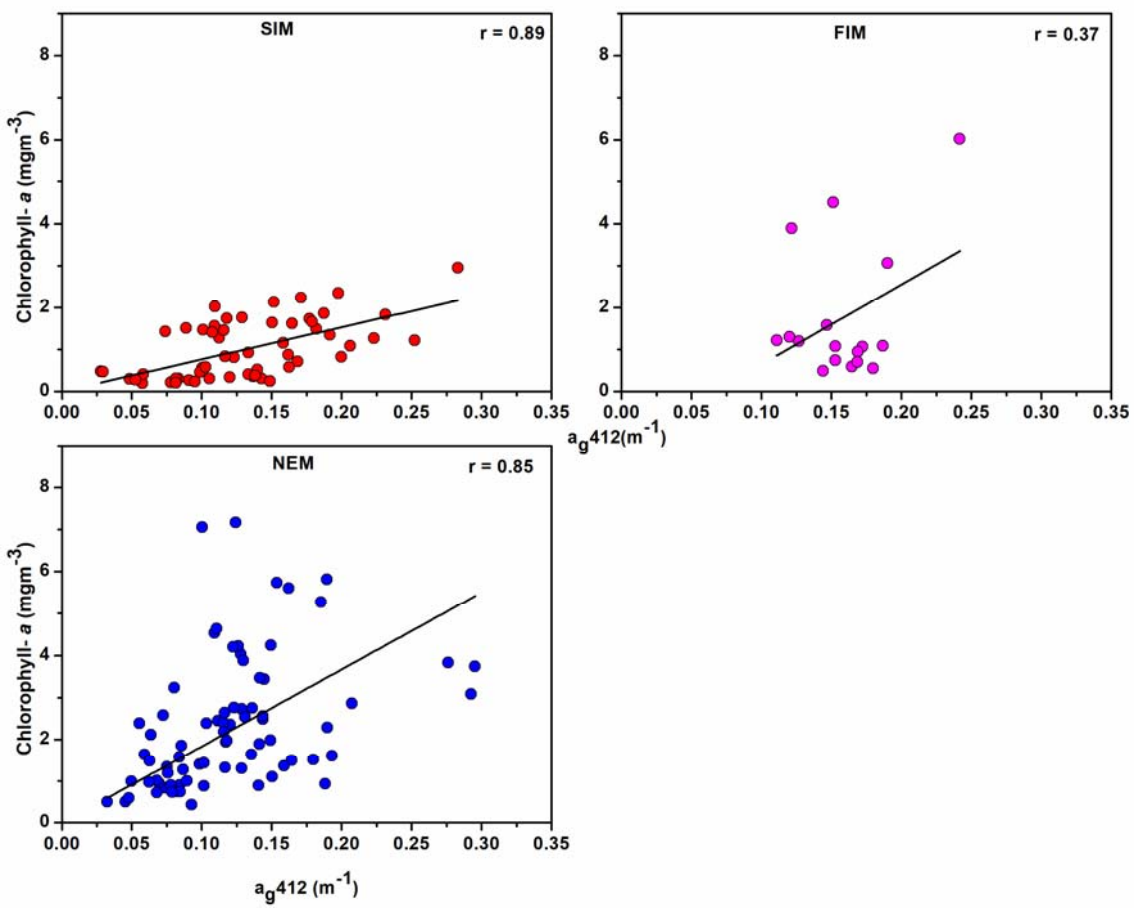
SIM
r = 0.89
FIM
r = 0.37
NEM
r = 0.85
Chlorophyll- a (mgm-3)
ag412(m-1)
ag412 (m-1)

Table 1: Seasonal variation of environmental and CDOM characteristics for the Mandovi and Zuari estuaries and the coastal waters of Goa.

Parameters	Season	Mandovi Estuary		Zuari Estuary		Coastal waters	
		Min	Max	Min	Max	Min	Max
Temp (˚C)	SIM	29.16	33.12	29.79	33.13	29.94	32.14
	SWM	24.40	33.16	26.39	29.78	No data	
	FIM	30.27	31.10	27.07	31.72	29.76	31.58
	NEM	26.78	30.06	26.62	30.28	26.60	29.85
Salinity	SIM	19.98	35.54	17.52	35.27	34.68	35.61
	SWM	0.06	35.52	0.05	28.08	No data	
	FIM	0.98	32.22	3.36	34.33	32.63	33.37
	NEM	5.43	34.72	8.44	34.76	33.61	35.27
Chlorophyll *a* (mgm^{-3})	SIM	1.25	16.14	0.71	11.10	0.311	3.02
	SWM	0.17	14.22	2.98	11.62	No data	
	FIM	0.7	3.4	1.35	8.06	0.59	1.58
	NEM	0.52	9.71	0.32	9.13	0.5	14.67
$a_{ph}676$ (m^{-1})	SIM	0.042	0.203	0.020	0.207	0.009	0.098
	SWM	0.002	0.198	0.027	0.136	No data	
	FIM	0.005	0.059	0.028	0.175	0.012	0.085
	NEM	0.025	0.138	0.018	0.174	0.009	0.136
a_g412	SIM	0.192	0.749	0.069	0.894	0.037	0.279
	SWM	0.193	0.842	0.263	1.458	No data	
	FIM	0.204	0.414	0.283	0.579	0.129	0.207

(m^{-1})	NEM	0.205	0.603	0.151	0.657	0.068	0.329
$S_{250-600}$ (nm^{-1})	SIM	0.0162	0.0194	0.017	0.0217	0.0145	0.0295
	SWM	0.0121	0.0203	0.0112	0.0174	No data	
	FIM	0.0148	0.0186	0.0131	0.0187	0.0168	0.022
	NEM	0.0156	0.0198	0.0135	0.0229	0.0169	0.027
$S_{275-295}$ (nm^{-1})	SIM	0.0187	0.0230	0.0191	0.0261	0.0230	0.0367
	SWM	0.0127	0.0241	0.0098	0.0187	No data	
	FIM	0.0143	0.0215	0.0141	0.0196	0.0239	0.0283
	NEM	0.0161	0.0233	0.0168	0.0248	0.0219	0.0327
S_R	SIM	1.053	1.572	0.976	1.488	1.442	2.363
	SWM	0.735	1.941	0.716	1.158	No data	
	FIM	0.860	1.267	0.858	1.489	1.430	1.690
	NEM	0.922	1.536	0.940	1.701	1.260	2.555

Supplementary Information

Figure S1: Spectral profiles of CDOM variations in the coastal (a - c) and estuarine waters (d - g) on a seasonal basis. Spectral profiles of rain water samples collected during 2015-16 are shown in h. The thick red line for the coastal and rainwater spectra indicates the average of all the values. The Mandovi Estuary is represented in green, while the Zuari Estuary in blue and the average of the spectra are shown in magenta and red colour respectively. Please note that the Y-axis for coastal and estaurine samples are different.

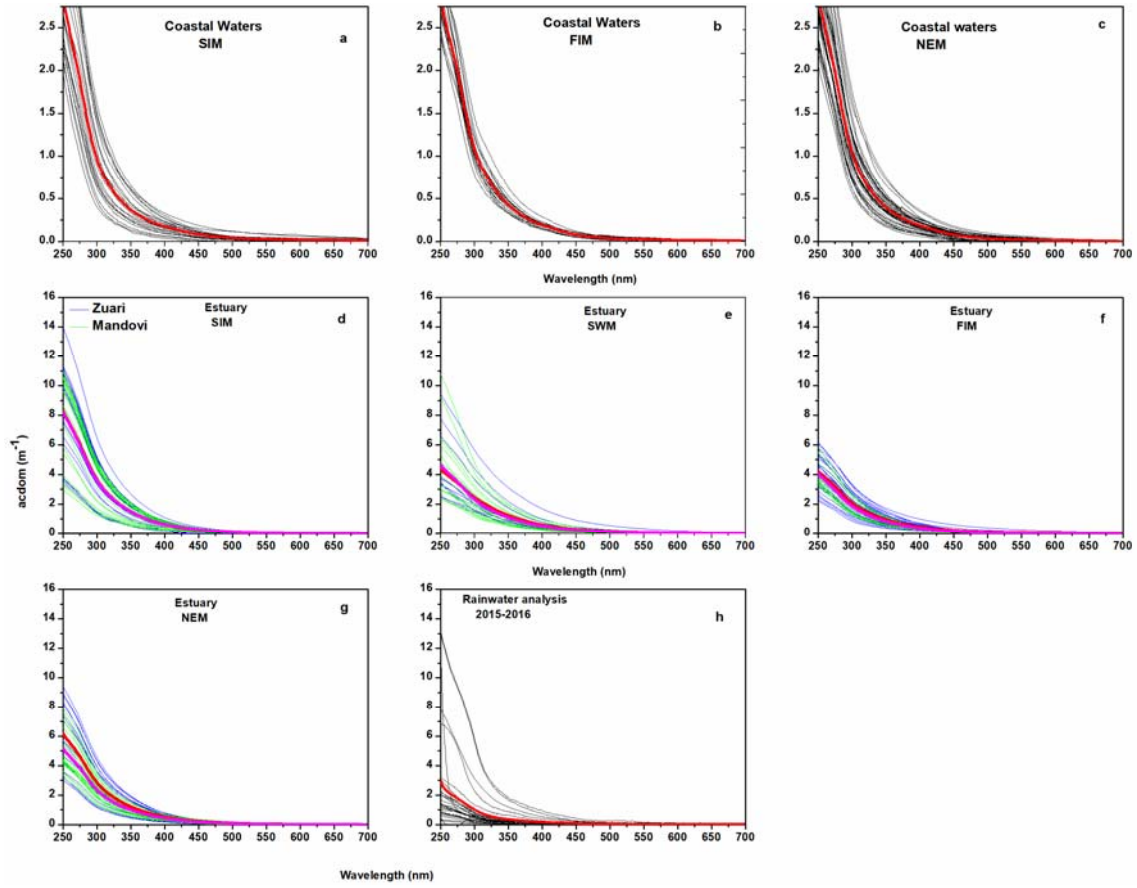

Figure S2: Spectral CDOM absorption during *Trichodesmium* bloom. The blooms were observed during the SIM (April - May) in the coastal waters off Goa during 2014 – 2017.

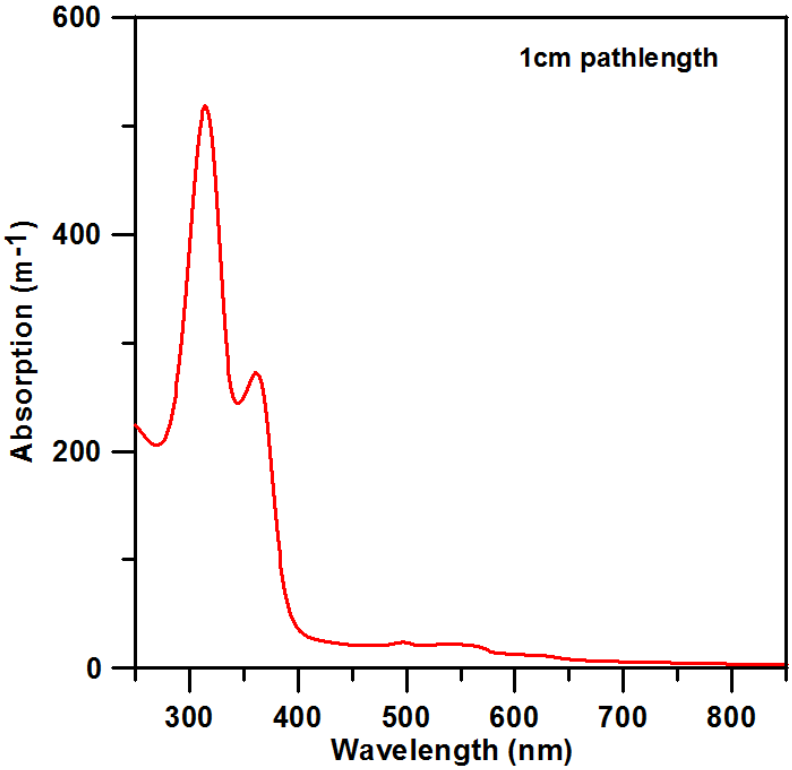

Figure S3: Relationship between daily average rainfall (mm) over the Goa region and CDOM absorption a_g412 (m^{-1}) in the Mandovi and Zuari estuaries.